Communications: Complete description of re-entrant phase behavior in a charge variable colloidal model system

Patrick Wette,[1,a)] Ina Klassen,[1] Dirk Holland-Moritz,[1] Dieter M. Herlach,[1] Hans Joachim Schöpe,[2] Nina Lorenz,[2] Holger Reiber,[2] Thomas Palberg,[2] and Stephan V. Roth[3]

[1]*Institut für Materialphysik im Weltraum, Deutsches Zentrum für Luft- und Raumfahrt (DLR), 51170 Köln, Germany*

[2]*Institut für Physik, Johannes Gutenberg Universität Mainz, Staudinger Weg 7, 55128 Mainz, Germany*

[3]*HASYLAB, DESY, Notkestraße 85, 22603 Hamburg, Germany*

(Received 11 December 2009; accepted 15 March 2010; published online 6 April 2010)

In titration experiments with NaOH, we have determined the full phase diagram of charged colloidal spheres in dependence on the particle density n, the particle effective charge Z_{eff} and the concentration of screening electrolyte c using microscopy, light and ultrasmall angle x-ray scattering (USAXS). For sufficiently large n, the system crystallizes upon increasing Z_{eff} at constant c and melts upon increasing c at only slightly altered Z_{eff}. In contrast to earlier work, equilibrium phase boundaries are consistent with a universal melting line prediction from computer simulation, if the elasticity effective charge is used. This charge accounts for both counterion condensation and many-body effects. © *2010 American Institute of Physics*. [doi:10.1063/1.3380823]

The phase behavior of charged colloidal spheres in aqueous suspension has attracted a lot of interest for their great potential use as model systems for the (classical) properties of metals.[1] Such Yukawa-like systems interact via a screened Coulomb potential can be varied over a wide range between the theoretical limits of the one component plasma and the hard sphere system.[2] The experimentally tunable parameters are the particle number density n, the concentration of screening electrolyte c, and the effective charge Z_{eff}. Early measurements focused on variations of n and c, reporting face centered cubic (fcc) structures at large n and later also body centered cubic (bcc) structures at low n and low salt conditions.[3–6] A complete phase diagram of the behavior at moderate to large c, covering also large n was measured by Sirota *et al.*[7] using ultrasmall x-ray scattering (USAXS). A glass phase was also reported for the first time for charged sphere colloids. In all these experiments, the bare particle charge Z stemming from particle synthesis was held constant. The influence of a variable charge is more subtle and was addressed less frequently. There are three main effects to be considered. Counterion condensation, self-screening, and many-body effects appearing as macroion shielding. A condensation of counterions at the particle surface occurs for large surface charge densities. Bucci *et al.*[9] were the first to demonstrate the implications for structure formation in an experimental study on in mixed micelles. They found that, consistent with theory,[8] the effective charge Z_{eff} would saturate at a certain value while Z was further increased[9] and no further gain of structure could be obtained. The effect was then elaborated by both theory[10] and experiment[11–14] and its interpretation as counterions condensation is generally accepted.[15] The corresponding number of free counterions is accessible from conductometry.[16,17] The phase behavior of Yukawa systems was first investigated with extensive computer simulations by Robbins, Kremer, and Grest (RKG), where a universal melting line for charged colloids was observed.[18] Later the study by Meijer and Frenkel (MF) (Ref. 19) leads to a melting line predicting a lower crystal stability compared to RKG whereas simulations by Hamaguchi *et al.*[20] gave results located between the ones of RKG and MF. Early studies of crystallization in charge variable systems[21] reported a good agreement with the RKG predictions. Later studies at larger bare charge, however, showed significant deviations toward a decreased crystal stability[5,22,23] when the charge from conductivity measurements was used. Moreover, upon charging up the particles by adding NaOH, the system first froze then remelted. This could only be partly explained as being due to an increased screening by the increase in the number of free counterions upon charging the particles (self-screening). The authors suggested like charge attraction and many-body effects as additional alternative explanations.

Recent experiments clearly favor the latter possibility. For a long ranged interacting two-dimensional charged sphere fluid, a significant reduction of repulsions was observed and attributed to macroion shielding.[24] The cage of nearest neighbors leads to a cutoff in the repulsion, as soon as the interaction range exceeds the nearest neighbor distance. This clear indication of many-body forces has since attracted considerable interest and drastic consequences for the phase behavior were predicted.[25,26] A comparison of the different experimentally and computationally accessible charge numbers was given by Shapran *et al.*[27] The effective charge under shielding conditions is given by measuring the elasticity of polycrystalline solids. To be specific, the motion of particles in a shear wave is described as harmonic oscillation within a potential created by the superposition of the potentials created by the neighboring hard-core Yukawa par-

a)Electronic mail: patrick.wette@dlr.de.

ticles up to the third coordination shell in a bcc lattice. In the absence of many-body effects such as shielding, the superimposed potentials are indeed safely assumed to be hard core Yukawa-like and an effective charge close to the effective conductivity charge is obtained. In the presence of shielding, however, the particle experiences a considerably less steep potential well. In this case, the interpretation in terms of hard core Yukawa potentials will yield a drastically lowered effective elasticity charge.

In fact, Wette and Schöpe[14] had shown that a consistent description of the phase transition for particles of constant bare charge Z is obtained, if this charge is used instead of the conductivity effective charge. Later Shapran *et al.*[28] found, from elasticity measurements along the phase boundary, indications of a transition from a condensation only to a condensation plus shielding regime upon decreasing n and c. At present, it is a completely open issue, whether this concept may also be applied to charge variable particles.

The present paper goes beyond previous studies in several ways. We perform a combined microscopy, light scattering, and USAXS study on the phase behavior of silica particles in dependence on n and the amount of added NaOH. We combine different ways to tune the particle interaction in one single system allowing a more reliable consistency check of the mean field description of charged colloidal crystal properties.[14] We confirm the re-entrant shape of the phase diagram from earlier studies[29] with much improved statistics and a qualitative extension to the regime of melting by the added electrolyte. In addition, we measure the elasticity effective charge of the polycrystalline solids along the phase boundaries and use these to compare to the theoretical expectations of RKG. We find a good agreement with the theoretical predictions *without* evoking like charge attraction arguments, when many-body effects are accounted for by using this elasticity effective charge.

Silica particles of diameter $2a=84$ nm were synthesized by Stöber synthesis and conditioned using an automated version of a closed-circuit conditioning setup reported earlier.[30] The peristaltically driven tubing circuit connects an ion exchange column, a reservoir under argon atmosphere to add water, particles, and NaOH, a conductivity cell to control the state of deionization and/or charging, the scattering cell and a cell to measure elasticity by torsional resonance spectroscopy for transparent samples of $n<60\ \mu\text{m}^{-3}$. It thus ensures identical interaction conditions for all measurements including the determination of the conductivity effective charge and the elasticity effective charge.[14] Fortunately, the polycrystalline solids are isotropic for length scales corresponding to the wavelength of the excited elastic waves and as we determine the orientationally averaged elasticity we may interpret our measured shear moduli in terms of an effective pair potential.[28] The cell is sealed from the preparation circuit by electromagnetic valves upon start of the structure measurements and the sample readily recrystallizes upon stop of shear. The phase behavior was determined at low n using standard static light scattering. At larger n, we performed USAXS measurements at the BW4-beamline at HASYLAB, Hamburg at a wavelength of $\lambda=0.138$ nm and a sample to detector distance of 13.3 m leading to a wide scattering vector range of $0.008\ \text{nm}^{-1}<q<0.280\ \text{nm}^{-1}$.

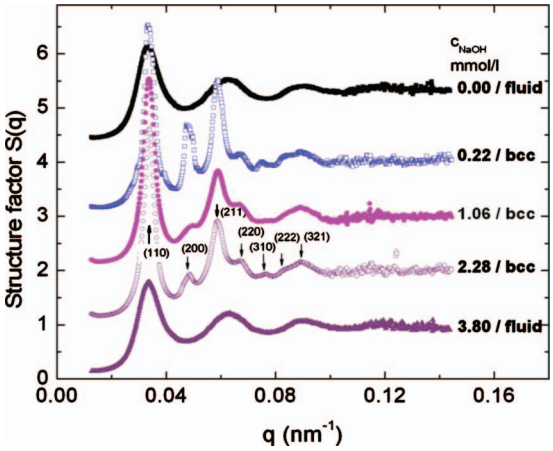

FIG. 1. USAXS static structure factors of the Si84 system measured at $n=113\ \mu\text{m}^{-3}$ and increasing concentrations of NaOH. Curves are shifted for clarity. From top to bottom: $c_{NaOH}=0$, 0.22, 1.06, 2.28, and 3.80 mmol/l. At the lowest and largest NaOH concentration, the sample shows a fluid structure while at medium concentrations a bcc polycrystalline structure is appearing as indicated by the Miller indices.

For radially averaged intensity $I(q)$, a conventional background and transmission correction was carried out before the structure factor $S(q)$ was calculated via $I(q)=I_0P(q)S(q)$, where $I_0P(q)$ is accessible at very large sodium hydroxide concentrations, c_{NaOH}, were particle interactions are sufficiently suppressed $(S(q)=1)$.[31]

Extracted USAXS static structure factors are shown in Fig. 1 for constant $n=113\ \mu\text{m}^{-3}$ and various c_{NaOH}. At low and large c_{NaOH}, the sample shows fluid structure, while at medium concentrations it forms a bcc polycrystalline structure as indicated by the miller indices. A fcc structure was not identified but is expected at higher particle concentration. The phase transition is clearly recognized by the appearance of crystalline peaks.

The full phase diagram is shown in Fig. 2. Upon increasing the concentration of NaOH the particles charge up via the reaction $\text{Si}-\text{OH}+\text{NaOH}\rightarrow\text{Si}-\text{O}^-+\text{Na}^+\text{H}_2\text{O}$. Bare charge Z, conductivity charge Z^*, and elasticity charge Z_{eff} increase. For sufficiently strong interaction, the system freezes, with the vertical bars denoting the coexistence region. The dashed line in the center of the crystalline region corresponds to the maximum effective charge Z_{eff} and coincides with minimum conductivity. Beyond the equivalence point the concentration of NaOH increases. At low pH the silica dissolves to form monosilicate at concentrations of about 1% w/w of the silica particles. Neglecting the small contribution of the monosilicates to the conductivity the excess concentration of NaOH is directly determined using Hessinger's model.[16] With increasing c_{NaOH}, the interactions become screened at only slightly decreasing charge and the system melts again. This effect differs from that observed by Yamanaka *et al.*,[22] who studied their sample only in a limited range of $6<p\text{H}<8$ with little excess NaOH and attributed their re-entrant behavior to the self screening effect upon charging. Here we have additional screening by the added electrolyte and hence may

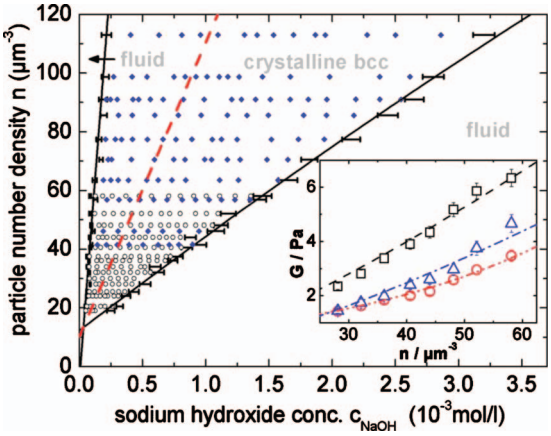

FIG. 2. Full phase diagram of charged silica (Si84) spheres in terms of the particle number density n (determined from the positions of the first peak of the structure factor) and the amount of added NaOH (determined from conductivity at known n) Open symbols denote microscopy and light scattering data, closed symbols denote USAXS data. The coexistence regions are indicated by horizontal bars. The system shows re-entrant melting due to charging (left boundary) and screening (right boundary). The central dashed line denotes the location of maximum interaction (largest shear moduli) which roughly coincides with the equivalence points of titration. The inset shows the shear moduli measured at different densities at the left phase boundary (up triangles) under condition of maximum interaction (squares) and at the right phase boundary (circles). The lines are fits to the data yielding $Z_{\mathrm{eff}}=253\pm15$ at the left phase boundary, $Z_{\mathrm{eff}}=340\pm20$ at maximum interaction and $Z_{\mathrm{eff}}=319\pm15$ at the right phase boundary.

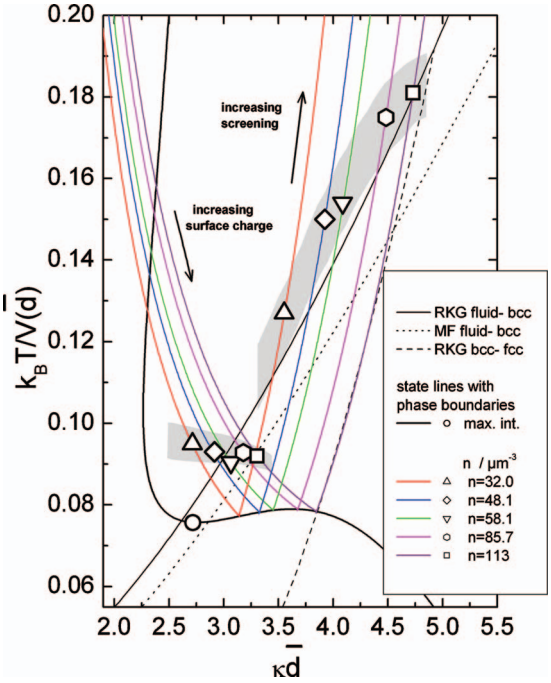

FIG. 3. Phase behavior of the charge variable silica spheres in the effective temperature-coupling strength plane as introduced by RKG (Ref. 18). The solid line denotes the universal melting line of RKG, the dotted line the later result of MF (Ref. 19), and the dashed line gives the bcc/fcc transition. The large symbols denote the experimentally observed melting transition(s) at maximum interaction with increasing n (circle) and at constant $n=32.0\ \mu\mathrm{m}^{-3}$ (up triangles), $48.1\ \mu\mathrm{m}^{-3}$ (diamonds), $58.1\ \mu\mathrm{m}^{-3}$ (down triangles), $85.7\ \mu\mathrm{m}^{-3}$ (hexagons), $113\ \mu\mathrm{m}^{-3}$ (squares) with increasing NaOH concentration. The melting points at both phase boundaries are surrounded by error regions (light gray areas) accounting for the uncertainties in Z_{eff}, c_{NaOH}, and n. The thin colored lines represent the corresponding state lines. At maximum interaction with increasing n, the corresponding state line was calculated using the maximum effective charge $Z_{\mathrm{eff}}=340$. The other state lines at constant n and increasing NaOH correspond to increasing surface charge (left state lines) and screening (right state lines).

investigate the dependence of the phase behavior for all three relevant interaction parameters.

To compare with the phase behavior predicted by computer simulation, we determined Z_{eff} along both phase boundaries and at maximum interaction from the shear moduli. The inset in Fig. 2 shows the results for increasing n. With the best fit applied to the respective data sets with a fitting procedure described in details elsewhere,[32] the mean effective charges were determined to be $Z_{\mathrm{eff}}=253\pm15$ at the left phase boundary, $Z_{\mathrm{eff}}=319\pm15$ at the right phase boundary and at maximum interaction we yield $Z_{\mathrm{eff}}=340\pm20$. At this state, the bare surface charge density of the Si84 system is $\sigma=3.4\ \mu\mathrm{C/cm}^{-2}$, which is much smaller than for previously used particles and corresponds to $Z=4500e$. It should be noted that elasticity charges are considerably smaller than corresponding conductivity charges Z_σ indicating the massive presence of macroion shielding.[32]

Using these values, we calculate the effective temperature $T^*=k_BT/V(\bar{d})$ and the coupling parameter $\lambda=\kappa\bar{d}$ via the screened Debye–Hückel potential $V(\bar{d})/k_BT=(Z_{\mathrm{eff}}^2\lambda_B)\times(\exp(\kappa a)/1+\kappa a)^2(\exp(-\kappa\bar{d})/\bar{d})$ with the Bjerrum length $\lambda_B=0.72$ nm, $\bar{d}=n^{-1/3}$, and the screening parameter $\kappa=\sqrt{4\pi k_BT\lambda_B(nZ_{\mathrm{eff}}+2\times10^3N_Ac_{\mathrm{NaOH}})}$, where the first term is the counterion concentration and the second accounts for the excess electrolyte. Ionic species stemming from the self-dissociation of water and from the monosilicate formation are neglected. This allows to construct the state lines for our sample in the effective temperature-coupling plane introduced by RKG (Ref. 18) (c.f. Fig. 3). We consider an increased n at maximum interaction (circles) and the charging and screening processes at different constant n and increasing NaOH concentration. By adding NaOH at constant particle number density, the surface charge and, due to this, the particle interaction $V(\bar{d})$ increases. The screening parameter κ is increasingly dominated by the particle counterions, while $\bar{d}$ is constant. Therefore the state lines decrease, cross the melting line, and encounter the maximum interaction state line as the surface charge reaches its maximum value. Further addition of NaOH increases the amount of excess electrolyte which screens the particle surface charge and therefore reduces particle interaction. κ is now dominated by the screening electrolyte leading to a monotonous increase of the state lines and they again cross the melting line. The large symbols on the state lines denote melting. In all cases, a good agreement with the theoretical expectation is observed. Thus one main result of the present study is the observation, that for charge variable particles the location of the melting transition can be precisely carried out, if effective charges which account for both counterion condensation and macroion shielding are used. In other words, many-body effects strongly influence the phase behavior of charged colloidal spheres.

A few remarks are at place. First, the maximum interaction state line does not show a pronounced maximum, rather

a saddle is observed and the melting line is crossed only once. This indicates graphically, that self-screening is much smaller than in previous studies. Our re-entrant behavior is due to excess electrolyte. Second, the data at the left phase boundary are close to both the original prediction of RKG and later results of MF.[19] Here within error bar, we cannot discriminate between these alternatives. Whereas the right phase boundary transition better coincides with the RKG prediction. Third, however, for small c_{NaOH} the melting points run nearly perpendicular to the fluid solid phase boundary and at large c_{NaOH} the data lie systematically short above the prediction. Both are attributed to the neglection of the contributions of monosilicate. Fourth, the largest concentration state line just touches the bcc/fcc melting transition, but evidence of this transition was neither gained from elasticity nor from scattering experiments. Possibly, this transition is encountered at larger n. Finally, we here used an approach different to that of some theoretical work[25,26] who corrected the universal melting line downward. Instead we used a reduced effective charge yielding elevated state lines and could reproduce the prediction of RKG.

We have shown that re-entrant melting can be observed in charge variable colloidal spheres due to first charging then screening of interactions occurring upon increasing the amount of added NaOH. We demonstrated that the observed transitions could be well described with a screened Coulomb repulsion, if not only counterion condensation (as predicted by charge renormalization theory[8,10,15]) but furthermore, also many-body effects by macroion shielding are accounted for, which are accessible via the orientationally averaged elasticity. For our case, we do not need to introduce like charge attractions discussed by other authors, as we observe a convergence between both effective charges neatly explained by a reduced repulsion range. We anticipate that in the long run a better modeling of the chemical processes occurring could even lead to a discrimination between different theoretical predictions based on purely repulsive interactions.

The authors like to thank J. Horbach for stimulating discussions and A. Timmann and S. Klein for experimental support. Financial support of the DFG (SPP1120, SPP1296, He1601/17, He1601/23, He1601/24, Pa459/12, Pa459/13, and Pa459/14), the MWFZ, Mainz, and the DLR, Cologne is gratefully acknowledged.

[1] D. Reinke, H. Stark, H.-H. von Grünberg, A. B. Schofield, G. Maret, and U. Gasser, Phys. Rev. Lett. **98**, 038301 (2007).
[2] A. Yethiraj, Soft Matter **3**, 1099 (2007).
[3] W. Luck, M. Klier, and H. Wesslau, Ber. Bunsenges. Phys. Chem. **67**, 75 (1963); **67**, 84 (1963).
[4] P. A. Hiltner and I. M. Krieger, J. Phys. Chem. **73**, 2386 (1969).
[5] Y. Monovoukas and A. P. Gast, J. Colloid Interface Sci. **128**, 533 (1989).
[6] T. Okubo, Prog. Polym. Sci. **18**, 481 (1993).
[7] E. B. Sirota, H. D. Ou-Yang, S. K. Sinha, P. M. Chaikin, J. D. Axe, and Y. Fujii, Phys. Rev. Lett. **62**, 1524 (1989).
[8] S. Alexander, P. M. Chaikin, P. Grant, G. J. Morales, P. Pincus, and D. Hone, J. Chem. Phys. **80**, 5776 (1984).
[9] S. Bucci, C. Fagotti, V. Degiorgio, and R. Piazza, Langmuir **7**, 824 (1991).
[10] L. Belloni, Colloids Surf., A **140**, 227 (1998).
[11] H. Versmold, U. Wittig, and W. Härtl, J. Phys. Chem. **95**, 9937 (1991).
[12] T. Gisler, S. F. Schulz, M. Borkovec, H. Sticher, P. Schurtenberger, B. D'Aguanno, and R. Klein, J. Chem. Phys. **101**, 9924 (1994).
[13] F. Bitzer, T. Palberg, H. Löwen, R. Simon, and P. Leiderer, Phys. Rev. E **50**, 2821 (1994).
[14] P. Wette and H. J. Schöpe, Prog. Colloid Polym. Sci. **133**, 88 (2006).
[15] E. Trizac and Y. Levin, Phys. Rev. E **69**, 031403 (2004).
[16] D. Hessinger, M. Evers, and T. Palberg, Phys. Rev. E **61**, 5493 (2000).
[17] J. Yamanaka, Y. Hayashi, N. Ise, and T. Yamaguchi, Phys. Rev. E **55**, 3028 (1997).
[18] M. O. Robbins, K. Kremer, and G. S. Grest, J. Chem. Phys. **88**, 3286 (1988).
[19] E. J. Meijer and D. Frenkel, J. Chem. Phys. **94**, 2269 (1991).
[20] S. Hamaguchi, R. T. Farouki, and D. H. E. Dubin, Phys. Rev. E **56**, 4671 (1997).
[21] T. Palberg, W. Mönch, F. Bitzer, R. Piazza, and L. Bellini, Phys. Rev. Lett. **74**, 4555 (1995).
[22] J. Yamanaka, H. Yoshida, T. Koga, N. Ise, and T. Hashimoto, Langmuir **15**, 4198 (1999).
[23] C. P. Royall, M. E. Leunissen, A. P. Hyinnen, M. Dijkstra, and A. van Blaaderen, J. Chem. Phys. **124**, 244706 (2006).
[24] R. Klein, H. H. v. Grünberg, C. Bechinger, M. Brunner, and V. Lobashkin, J. Phys.: Condens. Matter **14**, 7631 (2002).
[25] M. Brunner, J. Dobnikar, H. H. v. Grünberg, and C. Bechinger, Phys. Rev. Lett. **92**, 078301 (2004).
[26] A. P. Hynninen, M. Dijkstra, and R. v. Roij, Phys. Rev. E **69**, 061407 (2004).
[27] L. Shapran, M. Medebach, P. Wette, H. J. Schöpe, T. Palberg, J. Horbach, T. Kreer, and A. Chaterji, Colloids Surf., A **270–271**, 220 (2005).
[28] L. Shapran, H. J. Schöpe, and T. Palberg, J. Chem. Phys. **125**, 194714 (2006).
[29] J. Yamanaka, H. Yoshida, T. Koga, N. Ise, and T. Hashimoto, Phys. Rev. Lett. **80**, 5806 (1998).
[30] P. Wette, H. J. Schöpe, R. Biehl, and T. Palberg, J. Chem. Phys. **114**, 7556 (2001).
[31] S. V. Roth, R. Döhrmann, M. Dommach, M. Kuhlmann, I. Kröger, R. Gehrke, H. Walter, C. Schroer, B. Lengeler, and P. Müller-Buschbaum, Rev. Sci. Instrum. **77**, 085106 (2006).
[32] P. Wette, H. J. Schöpe, and T. Palberg, J. Chem. Phys. **116**, 10981 (2002).